Enhanced giant magnetoresistance in magnetic/nonmagnetic $La_{1-x}MnO_{3-\delta}$ oxide multilayers

S. Sundar Manoharan, K. M. Satyalakshmi, V. Prasad†, S. V. Subramanyam† and M. S. Hegde‡

Solid State and Structural Chemistry Unit, Department of Metallurgy, †Department of Physics, Indian Institute of Science, Bangalore 560 012, India

Over 80% negative giant magnetoresistance (GMR) is observed in the self doped $La_{0.7}Mn_{3-\delta}$ oxide thin film in a magnetic field of 6 Tesla at 225 K. $La_{0.7}Mn_{3-\delta}$ (magnetic)/$La_{0.85}MnO_3$ (nonmagnetic) oxide multilayers showed a higher GMR effect up to 89% at 225 K compared to the single $La_{0.7}Mn_{3-\delta}$ oxide films. The results demonstrate that the large GMR observed in the doped manganates is inherent to the oxide material whereas the enhanced GMR to the extent of 6–10% in the multilayers compared to the parent magnetic film is due to the coupling of magnetoresistance in the parallel magnetic oxide layers separated by nonmagnetic oxide layers as in $(Fe/Cr)_n$ multilayer metal film.

GIANT magnetoresistance (GMR) is defined by the ratio $(R_H - R_0)/R_0$, where R_H and R_0 are the resistances in presence and absence of a magnetic field. GMR effect was first observed in the single crystals of $La_{0.62}Pb_{0.38}MnO_3$[1]. Over 50% negative GMR was reported by Baibich *et al.*[2] in $(Fe/Cr)_n$ magnetic/nonmagnetic metal multilayers. Presently, there is a tremendous interest in the study of GMR effect because, large variation in the resistance in the presence and absence of a magnetic field can have direct application as the 'readhead' for magnetic recording systems. Observation of over 50% GMR in the epitaxial thin films of $La_{0.67}Ba_{0.33}MnO_3$ oxide thin films[3] at 300 K triggered the interest on this subject. $La_{1-x}M_xMnO_3$ (M = Ca, Sr, Pb)[4–6] thin films showed large GMR effects.

$LaMnO_3$ is an antiferromagnetic oxide possessing orthorhombic structure. It is possible to synthesize lanthanum deficient $La_{1-x}MnO_3$ with 18–20% Mn ions in the 4+ state. These compounds crystallize in a rhombohedral structure and exhibit a paramagnetic to ferromagnetic transition, coupled with insulator to metal transition, when samples are cooled below 300 K. We have recently observed over 80% GMR in 5% Ag-doped $La_{0.7}MnO_{3-\delta}$ thin films at 220 K.

Although large GMR effect is observed in the doped manganates, it is not yet clear whether the mechanism of GMR operating in these oxide films is the same as in the $(Fe/Cr)_n$ multilayer metal films. In order to gain further insight into the mechanism of GMR we considered it worthwhile to fabricate $La_{0.7}MnO_{3-\delta}$ (magnetic)/$La_{0.85}MnO_{3-\delta}$ (nonmagnetic) oxide multilayers since they are structurally compatible. We report, in this paper, the first fabrication of magnetic/nonmagnetic oxide multilayers by pulsed laser deposition and show an enhanced GMR effect in the oxide multilayers compared to the parent $La_{0.7}MnO_{3-\delta}$ magnetic oxide thin films.

Bulk samples of nominal composition $La_{0.7}MnO_{3-\delta}$ and $La_{0.85}MnO_{3-\delta}$ were prepared by heating stoichiometric amounts of La_2O_3 and $MnCO_3$ at 1050°C in air. These oxides in bulk did show ferromagnetic transition at 220 and 240 K, respectively. However, when the films of these materials were made by pulsed laser deposition, they did not show metallic transition. The discrepancy in the properties of the bulk solid and the thin films was attributed to oxygen deficiency. In order to overcome the oxygen out-diffusion in the thin films, 5% Ag_2O was added to the $La_{0.7}MnO_{3-\delta}$ which was used as the laser target. Silver is known to enhance epitaxial growth of $YBa_2Cu_3O_{7-\delta}$ films in addition to bringing in extra oxygen during pulsed laser deposition[8]. Ag ion is not known to substitute for any ion in $La_{1-x}MnO_3$. The films grown with 5% Ag_2O showed metallic conductivity below 220 K. Films made out of $La_{0.85}MnO_{3-\delta}$ pellet (without addition of Ag_2O) showed a semiconducting behaviour which is employed as the nonmagnetic oxide layer in this study.

Thin films of $La_{0.7}MnO_{3-\delta}$ with 5% Ag_2O (Ag-MNO) and $La_{0.85}MnO_{3-\delta}$ (LMO) without Ag_2O were deposited separately on $LaAlO_3$ (1 0 0) substrate by pulsed laser deposition at 720°C in 300 mtorr O_2. Superlattices of $(Ag–LMO/LMO)_{20}$ were also deposited on $LaAlO_3$ (1 0 0) substrate. Ag–LMO and LMO were deposited alternatively using a multitarget holder with 60 and 12 laser pulses, respectively, at a (KrF 248 nm) laser pulse energy density of 2 J/cm^2. From the thicknesses of Ag–LMO and LMO films prepared separately, estimated layer thicknesses in the multilayer are 100 Å and 20 Å, respectively, for Ag–LMO and LMO. X-ray diffraction pattern of the multilayer film given in Figure 1 shows highly textured growth in (1 0 0) direction on $LaAlO_3$ with pseudocubic $a = 3.88$ Å agreeing well with the observed a parameter of the bulk $La_{1-x}MnO_{3-\delta}$. Ag–LMO as well as LMO films also showed a similar oriented growth. Superlattice reflections were not seen in the form of satellite peaks adjacent to (1 0 0) or (2 0 0) reflections of LMO possibly because La^{3+} and oxygen defects are randomly distributed.

Resistivity measured by four point probe method at zero field for a 2500 Å thick epitaxial film of Ag–LMO, LMO and $(Ag–LMO/LMO)_{20}$ multilayer are shown in Figure 2. Sharp change in the slope is observed in the ρ vs T curve, for the Ag–LMO and the multilayer films. The LMO film showed a semiconducting behaviour. Room temperature resistivity of Ag–LMO and LMO

‡For correspondence.

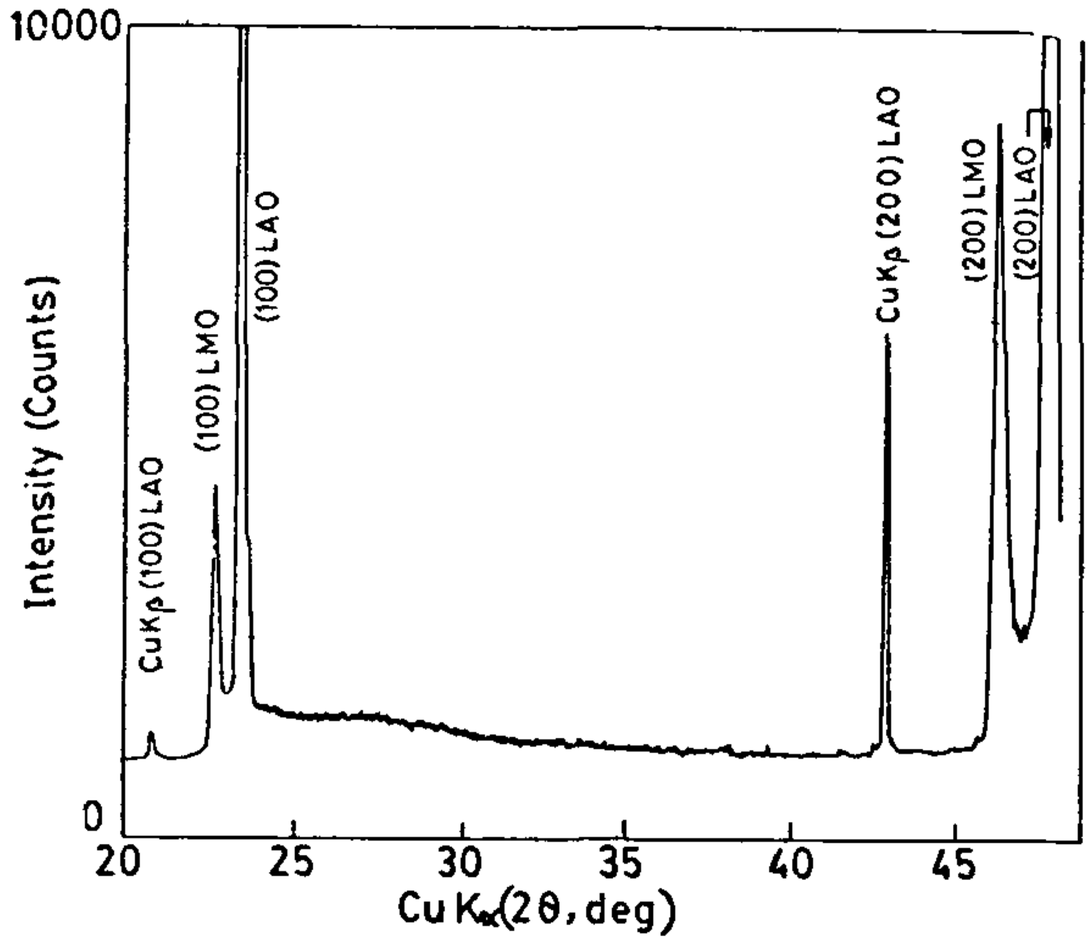

Figure 1. X-ray diffraction pattern of (Ag–$La_{0.7}MnO_{3-\delta}$/$La_{0.85}MnO_{3-\delta}$)$_{20}$ multilayer thin film.

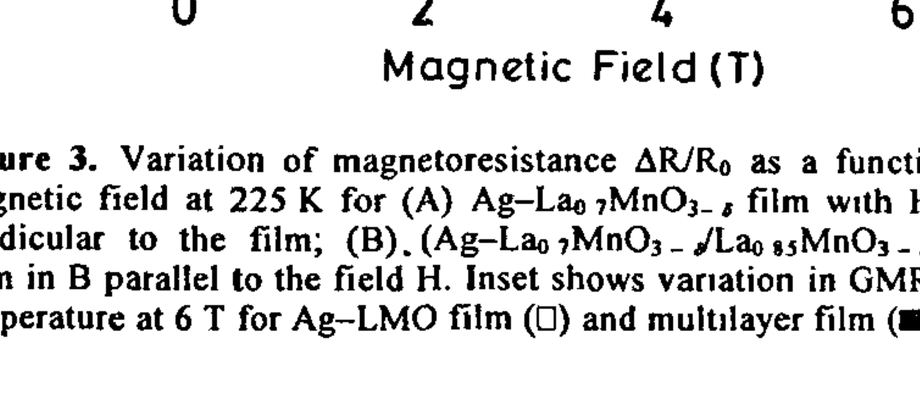

Figure 3. Variation of magnetoresistance $\Delta R/R_0$ as a function of magnetic field at 225 K for (A) Ag–$La_{0.7}MnO_{3-\delta}$ film with H perpendicular to the film; (B) (Ag–$La_{0.7}MnO_{3-\delta}$/$La_{0.85}MnO_{3-\delta}$; (C) Film in B parallel to the field H. Inset shows variation in GMR with temperature at 6 T for Ag–LMO film (□) and multilayer film (■)

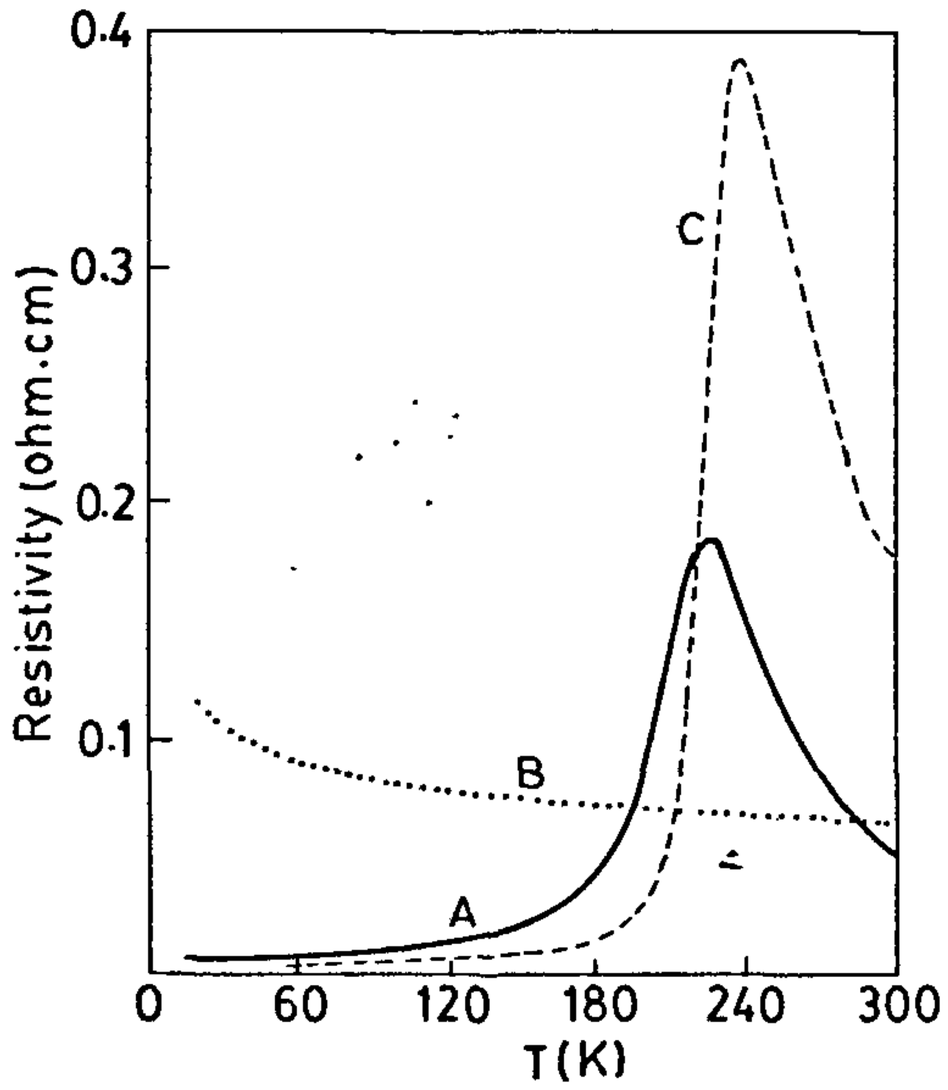

Figure 2. Resistivity vs temperature plots of (A) Ag–$La_{0.7}MnO_{3-\delta}$, (B) $La_{0.85}MnO_{3-\delta}$ and (C) (Ag–$La_{0.7}MnO_{3-\delta}$/$La_{0.85}MnO_{3-\delta}$)$_{20}$ multilayer films on $LaAlO_3$ (100).

films were in the range of 60–70 mΩ cm. Metal to insulator transition temperature, T_c in the multilayer film is about 235 K and that in the single Ag– $La_{0.7}MnO_{3-\delta}$ film is 225 K. The higher resistivity of the multilayer film above 220 K can be accounted for in terms of addition of resistances of the Ag–$La_{0.7}MnO_{3-\delta}$ and $La_{0.85}MnO_{3-\delta}$ films in series. Below the transition temperature the metallic resistivity of Ag–LMO dominates and resistivity of the film is essentially a parallel combination of the two oxide layers.

In Figure 3 are shown the percentage $\Delta R/R_0$ vs magnetic field, plots for the parent Ag–LMO (A) and (Ag–LMO/LMO)$_{20}$ (B) multilayer films at 225 K. The measurements were made with H parallel and perpendicular to the film surface. In the case of the parent Ag–LMO film, about 80% GMR is obtained at 6T and there was no difference in the GMR values whether H was parallel or perpendicular to the film surface. A similar isotropic GMR effect is reported in all the doped lanthanum manganate films[3–6]. An enhanced GMR effect is observed in the (Ag–LMO/LMO)$_{20}$ film by about 6–10% compared to the parent Ag–LMO. Further, when the H was parallel to the surface, GMR value was higher by 3% compared to when H was perpendicular (curve C). Anisotropic GMR effect was observed in the case of $(Fe/Cr)_n$ metallic multilayer film as well. In the inset, GMR vs T plots for the parent and multilayer films measured at 6 T parallel to the film surface is shown demonstrating the enhanced GMR effect in the multilayer films.

The pseudocubic cell of doped manganates in general consists of MnO_2 magnetic layers separated by a nonmagnetic La–O or La(M)–O (M = divalent ion) oxide layers. As the temperature is decreased, ferromagnetic order sets in the MnO_2 layer due to Zener double exchange mechanism of electron transfer in the Mn^{3+}–O–Mn^{4+} chains in all the three directions and resistivity

decreases[9,10]. Alternatively, when a magnetic field is applied externally at a given temperature, ferromagnetic order is induced in the MnO_2 layers leading to a decrease in resistance. In the self doped $La_{0.7}MnO_{3-\delta}$, the pronounced GMR effect is attributed to La^{3+} and O^{2-} vacancies which form the scattering centers for the conducting electrons, thereby increasing the resistivity. Applied magnetic field seems to provide sufficient activation energy for the alignment of spins to overcome the additional scattering of conducting electrons.

In the case of multilayer, we propose that there are two factors contributing to the total GMR. The first one is the decrease in the resistances of individual magnetic oxide layers as in the single Ag–LMO film. This value is about 80% at 6T. The second factor is the parallel combination of resistances of the individual magnetic oxide layers separated by the non-magnetic spacer layer. This is about 8–10% thus giving 89% GMR at 6T in the $(Ag–LMO/LMO)_{20}$. The secondary contribution seems to arise from the spin dependent scattering of the conduction electrons at the interface between the ferromagnetic oxide and the nonmagnetic oxide. The order of magnitude of the secondary contribution to the total GMR is about 8–10% which is about the same as that of magnetic/nonmagnetic metal multilayers such as $(Co/Cu)_n$.

In conclusion, we have shown for the first time, a superlattice sequence of magnetic/nonmagnetic oxide multilayer, mimicking the $(Fe/Cr)_n$ superlattices, showing an enhanced GMR compared to the GMR observed in the parent magnetic oxide thin films. We have also shown an anisotropic behaviour in the multilayer oxide films compared to an isotropic behaviour in lanthanum manganate thin films,

1. Searle, C. W. and Wang, S. T., *Can. J. Phys.*, 1970, **48**, 2023–2031.
2. Baibich, M. N , Broto, J. M , Fert, A., Nguyen Van Dau, F., Petroff, F., Etinne, P., Creuzet, G., Fredrick, A. and Chazelas, J., *Phys. Rev. Lett* , 1988, **61**, 2472–2475.
3. von Helmolt, R., Wecher, J., Holzafel, B , Shultz, L. and Samwer, K., *Phys. Rev. Lett.*, 1993, **71**, 2331–2333.
4. Chahara, K. I., Ohno, T., Kasai, M. and Kozono, Y., *Appl. Phys. Lett.*, 1993, **63**, 1990–1992.
5. Ju, S. L., Kwon, C., Li, Q., Greene, R. L. and Venkatesan T., *Appl. Phys. Lett.*, 1994, **65**, 2108–2110.
6. Sundar Manoharan, S., Vasanthacharya, N. Y., Hegde, M. S , Satyalakshmi, K. M., Prasad, V. and Subramanyam, S. V., *J. Appl. Phys.*, 1994, **76**, 3923–3925.
7. Sundar Monoharan, S., Dhananjay Kumar, Hegde, M. S., Satyalakshmi, K. M , Prasad, V. And Subramanyam, S. V , *J. Solid State Chem.* (in press).
8. Dhananjay Kumar, Satyalakshmi, K. M., Sundar Monoharan, S. and Hegde, M. S., *Bull. Mater. Sci.*, 1994, **67**, 625–632
9. Goodenough, J. B., *Progr. Solid State Chem.*, 1971, **5**, 149–350
10. Mahesh, R., Mahendiran, R., Raichaudhury, A. K. and Rao, C. N. R., *J. Solid State Chem.*, 1995, **114**, 297–299.

ACKNOWLEDGEMENTS. We thank the Department of Science and Technology, Government of India, for financial assistance. KMS thanks CSIR for a senior research fellowship.

Received 31 March 1995; revised accepted 10 July 1995

Physiobiochemical aspects of development of hardseededness in *Albizia lebbek*

R. C. Uniyal and A. R. Nautiyal

High Altitude Plant Physiology Research Centre,
HNB Garhwal University, Srinagar Garhwal 246 174, India

Seeds of *Albizia lebbek* exhibit dormancy due to hard seeded coat. Seed development was studied in this species to determine whether the induction of hardseededness precedes or succeeds the attainment of physiological maturity and also whether the hardseededness is an inherent character of the seed or can be escaped by harvesting seeds before its induction. The seeds attained physiological maturity at approximately 230 DAA accompanied by acquisition of germinability. This phase was characterized by rapid accumulation of starch, soluble carbohydrates, proteins and chlorophyll. The onset of hardseededness followed, proceeding gradually until 270 DAA and then increased rapidly. While the soluble carbohydrates and chlorophyll contents declined during this period, the starch and proteins showed an increase. Hardseededness in these seeds seems to be their inherent character as it not only occurred in seeds attached to the parent plant but also in seeds in storage, although considerably delayed in the latter case.

DELAYED germination of seeds due to hard seed coats is a common characteristic of many leguminous seeds. *Albizia lebbek* (L.) Willd. is one such multipurpose tree species in which hardseededness poses a practical problem for germination of its seeds. The occurrence of hardseededness in some seeds indicates that the prevailing environment during seed development plays a significant role in developing a hard seed coat[1–3]. However, information is lacking on the germinability and performance of seeds harvested prior to induction of hardseededness. Thus, the present investigation was undertaken to determine whether seeds attain germinability before the induction of hardseededness, and if so, whether hardseededness could be escaped by harvesting seeds before its induction.